

## Supporting Information

Title: Self-assembly based plasmonic nanoparticle arrays coupling with hexagonal boron nitride nanosheets

Wei Gao, Yan Zhao, Hong Yin,\* and Hong-Dong Li

S1: The dispersion of BNNSs in ethanol and DI water solutions.

The as-exfoliated BNNSs are solid powder-like samples after centrifugation, cleaning, and drying process. We re-dissolved these BNNSs into DI water and ethanol solvents, forming homogeneous h-BN nanosheets dispersions with the concentration of 4mg/15mL. Figures S3(a-d) demonstrate the photographs of BNNSs dispersed in ethanol and DI water solvents after ultrasonication with the different storage time. As can be clearly observed that these solvents afforded light white and semi-transparent with “milky” appearances until 24 h. Figure S3(e-h) are the photographs of BNNSs dispersions in ethanol and DI water solutions bearing a laser beam from left side as well as figures S3(i-l) are the photographs of BNNSs dispersions in the same solutions bearing a laser beam from the right side. The path of a laser beam could be clearly observed through the dispersion due to the scattering of the h-BN nanosheets. The occurrence of the Tyndall effect of the diluted dispersion in ethanol and DI water reveals the colloidal nature of the dispersion. These dispersions were very stable with small levels of sedimentation over a period of 24 h. Furthermore, after 24 h the milky appearance became less significant, and dispersions appeared more transparent probably due to the inter-nanosheets aggregation associated with gradual decomplexation. Nevertheless the Tyndall effect can be observed after 36 h indicating the good dispersion of h-BN nanosheets.

S2 : Atomic Force Microscopy (AFM)

The thicknesses of the exfoliated sheets were measured by AFM. The samples for AFM were prepared by drop casting the exfoliated BNNSs on Silicon wafer. This induced the flakes to stack on top of each other as it can be seen in Figure S1. The different spots that were analyzed shows that the sheets are stacked layer by layer. The thickness for these sheets were 2.38 nm, 2.70 nm and 3.47 nm, which are 4-8 layers of atomic thin h-BN considering previously reported AFM thickness (0.4-0.5 nm for monolayer, 0.8-0.9 nm for bi layer and 1.2-1.3 nm for three layer system).

### S3: Scanning Electron Microscopy (SEM) and Energy Dispersive X-ray Spectroscopy (EDX)

The Au NP arrays formed by annealing were characterized by SEM and EDX measurements. The micellar Au NP arrays were dip-coated on a Silicon wafer and subsequently annealed at 500 °C for 20 min to remove the polymer matrix. The sample was measured by SEM and EDX before and after annealing. SEM images of Au NPs before and after annealing as shown in Figure S2 a and b suggests that the particle is fabricated and remains their local positions. EDX was utilized to monitor the carbon content that is the main elemental consists in polymer matrix. As shown in Figure S2 c and d, carbon content is dramatically reduced after annealing process below the detection limit.

### S4: Au NPs anchored to BNNS surfaces.

The as-synthesized BNNSs are added into the different micelle solutions which have been pre-loaded with Au salts. The resulting BNNS/Au NP composites are dip-coated on silicon substrates followed an annealing step at 500 °C for 20 mins. This annealing temperature is well below the reported critical temperature (840 °C) for BNNS with 1-4 atomic layers sustain in air.<sup>1</sup> EDX results show that the carbon content is dramatically reduced after annealing process, suggesting the polymer matrix is removed by annealing step. Thus, Au NPs are expected to be anchored to the surfaces of exfoliated BN nanosheets. Figs. S4(a-d) display SEM images with high magnification of 9 nm Au NPs decorated on BNNS surfaces for different samples. It can be observed that the Au NPs distribute homogeneously onto the surfaces of BNNSs without any agglomeration, even in the wrinkle regions (marked in the red circle areas in SEM images). Furthermore, the hexagonal distribution of Au NPs is almost remained.

On the other hand, the electronic structures of BNNS-Au NPs hybrid composites have been investigated by X-ray photoelectron spectroscopy (XPS) measurements. Figure S5 shows the XPS survey spectra of BNNSs with and without Au NPs. B 1s, N 1s, O 1s, Si 2s and 2p peaks can be seen from the survey scan for the pure BNNSs. After decoration of Au NPs, the intensity of B 1s and N 1s peaks are dramatically reduced whileas that of Si 2s and 2p increase significantly. This is mostly likely due to the oxidation of Si substrate resulting from the annealing step. A pronounced Au 4f peak is observed for the BNNSs with Au NPs, while it is absent in the counterpart without Au NPs. This suggestes that Au was indeed incorporated into the resultant BNNSs. Since the annealing temperaure is reasonalbly lower than the critical oxidation temperature of BNNSs, B 1s and N 1s were traced by the core level scans for the BNNS-Au NPs composites in Figure S5(b) and (c). Generally, N 1s peak at 398

eV is commonly found for BNNSs with and without Au NPs. However, a shoulder peak at relatively high binding energy of N 1s is found for the sample with Au NPs, suggesting a  $\pi$  conjugated system. The polar, core-forming P2VP block contains N atoms in the aromatic rings, and atomically thin BN has a strong absorption capability toward aromatic molecules due to  $\pi-\pi$  interactions.<sup>2</sup> Au 4f core level spectrum in Figure S5(d) shows 4f<sub>7/2</sub> and 4f<sub>5/2</sub> locating at 83.7 and 87.3 eV, respectively, corresponding to the metallic Au. Again, this suggests that Au in micelles is reduced due to the annealing process.

1. Q. Cai, D. Scullion, A. Falin, K. Watanabe, T. Taniguchi, Y. Chen, E. J. G. Santos and L. H. Li, *Nanoscale*, 2017, **9**, 3059-3067.
2. Q. Cai, S. Mateti, K. Watanabe, T. Taniguchi, S. Huang, Y. Chen and L. H. Li, *ACS Appl. Mater. Interfaces*, 2016, **8**, 15630-15636.

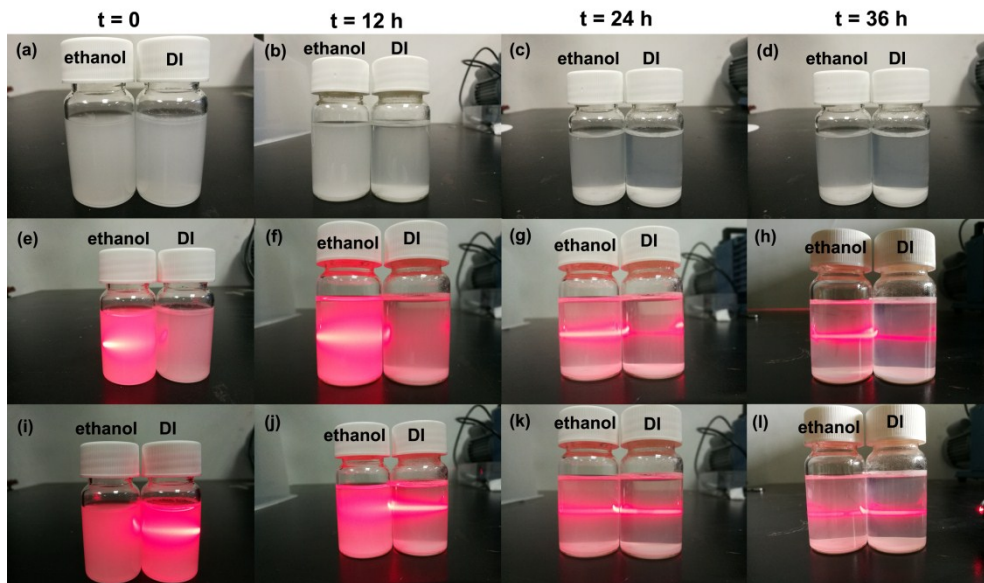


**Fig. S1** (a-d) Photographs of exfoliated BNNs dispersed in ethanol (left) and DI water (right) solutions with different storage time; (e-h) are the photographs of the same solutions with the irradiation of a laser beam from the left; (i-l) are the photographs of the same solutions with the irradiation of a laser beam from the right;

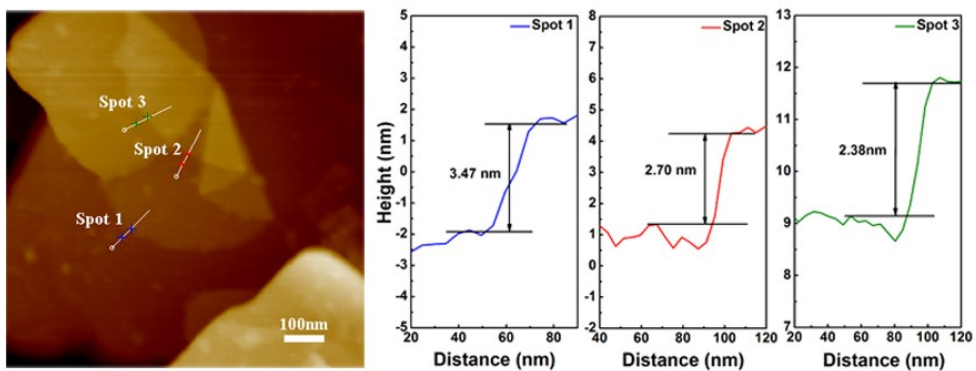


**Fig. S2** AFM image of typical exfoliated BNNSs and the corresponding height profiles at different spots.

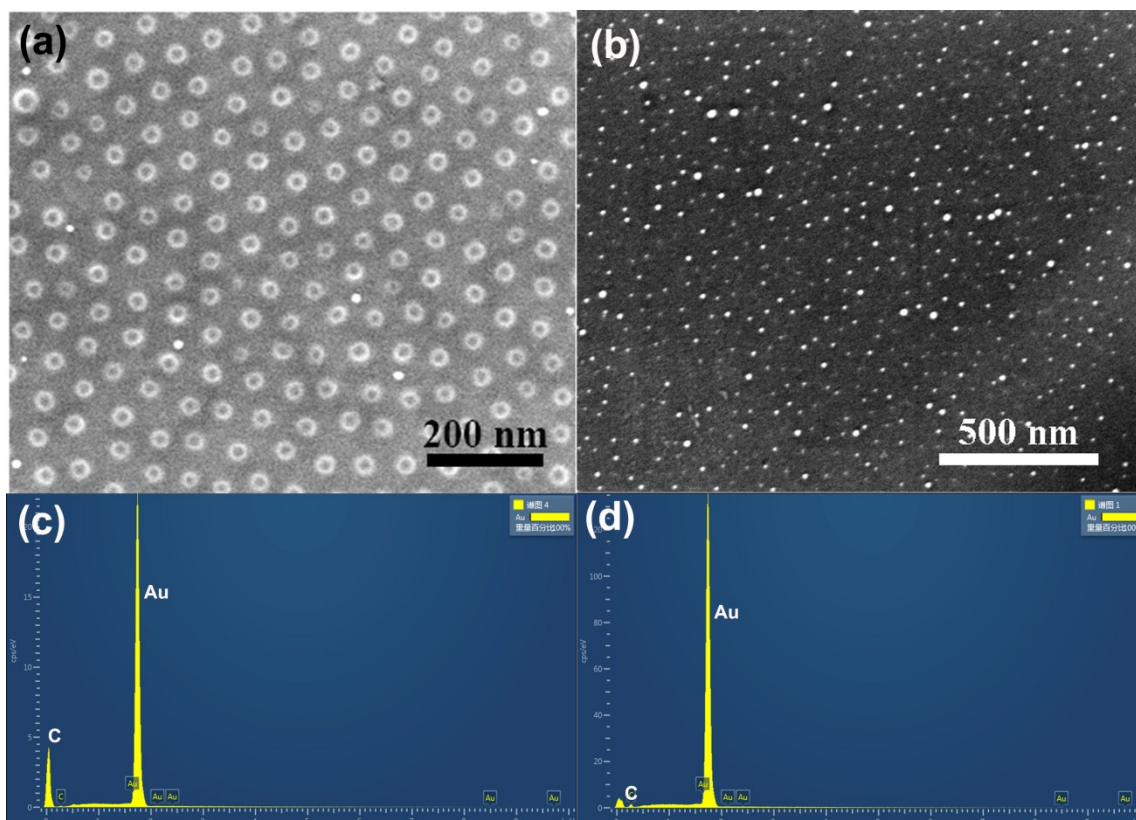


**Fig. S3** SEM images micellar Au NP arrays before (a) and after (b) annealing and the corresponding EDX results before (c) and after (d) annealing.

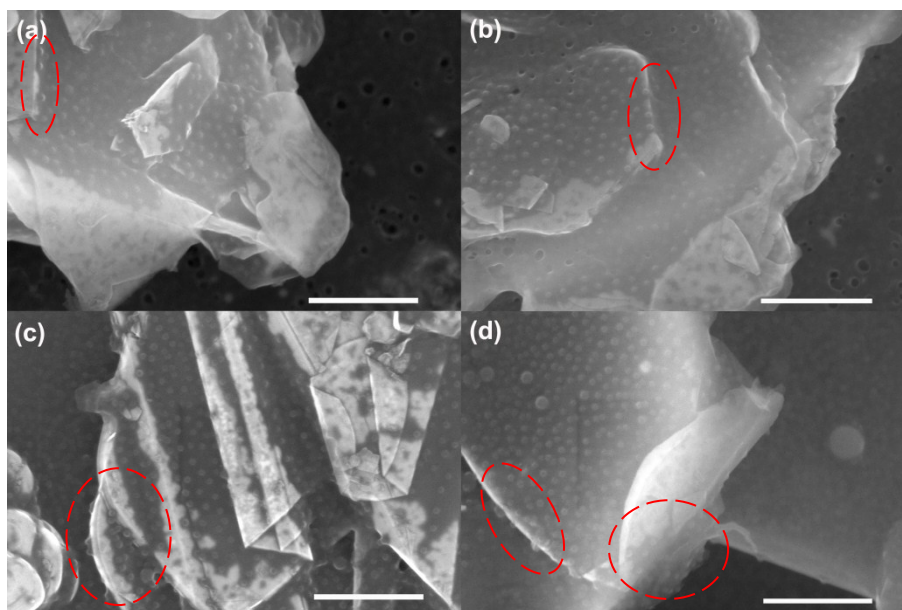


**Fig. S4** SEM images of BNNs-Au NPs hybrid materials. The red circles mark the wrinkles of BNNs with Au NPs sustained.

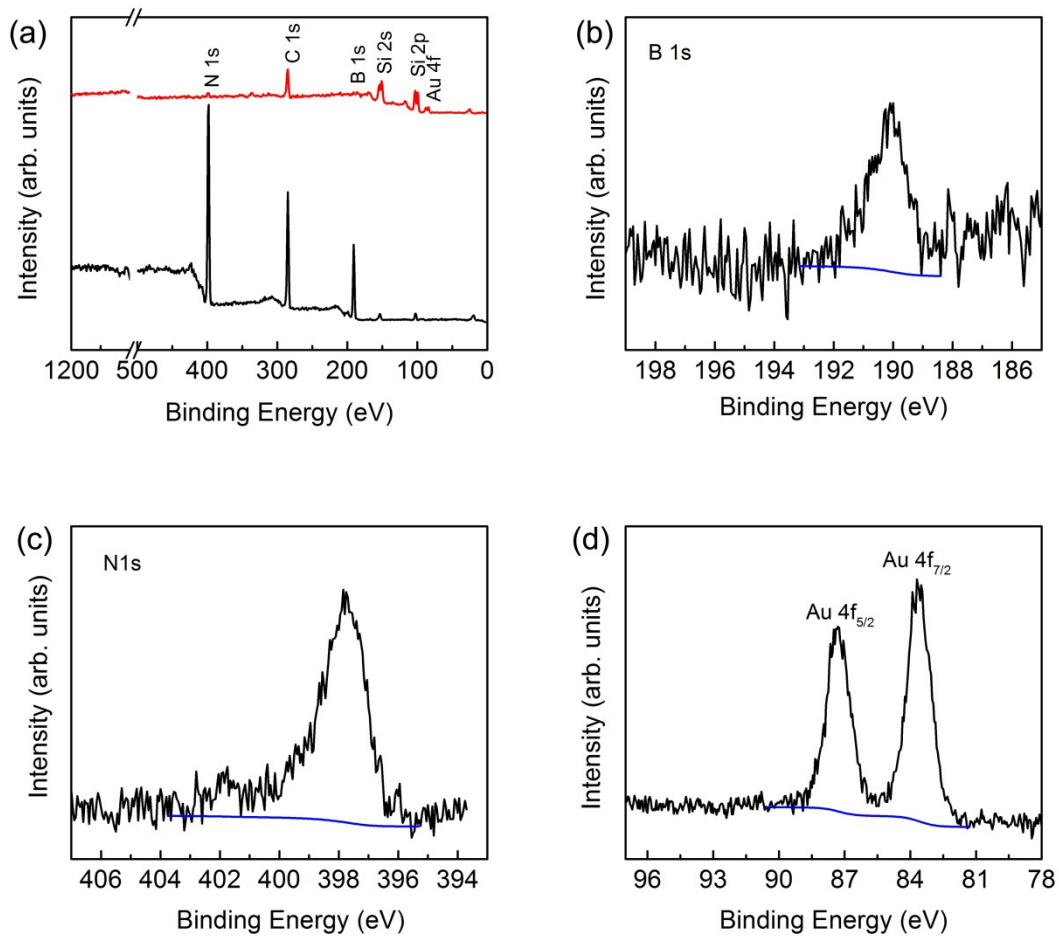


**Fig. S5** (a) XPS survey spectra of BNNSs with (upper curve) and without (lower curve) Au NPs decoration; XPS core level spectra of (b) B 1s, (c) N 1s and (d) Au 4f for BNNSs with Au NPs decoration.